

An impenetrable barrier to ultrarelativistic electrons in the Van Allen radiation belts

D. N. Baker¹, A. N. Jaynes¹, V. C. Hoxie¹, R. M. Thorne², J. C. Foster³, X. Li¹, J. F. Fennell⁴, J. R. Wygant⁵, S. G. Kanekal⁶, P. J. Erickson³, W. Kurth⁷, W. Li², Q. Ma², Q. Schiller¹, L. Blum¹, D. M. Malaspina¹, A. Gerrard⁸ & L. J. Lanzerotti⁸

Early observations^{1,2} indicated that the Earth's Van Allen radiation belts could be separated into an inner zone dominated by high-energy protons and an outer zone dominated by high-energy electrons. Subsequent studies^{3,4} showed that electrons of moderate energy (less than about one megaelectronvolt) often populate both zones, with a deep 'slot' region largely devoid of particles between them. There is a region of dense cold plasma around the Earth known as the plasmasphere, the outer boundary of which is called the plasmopause. The two-belt radiation structure was explained as arising from strong electron interactions with plasmaspheric hiss just inside the plasmopause boundary⁵, with the inner edge of the outer radiation zone corresponding to the minimum plasmopause location⁶. Recent observations have revealed unexpected radiation belt morphology^{7,8}, especially at ultrarelativistic kinetic energies^{9,10} (more than five megaelectronvolts). Here we analyse an extended data set that reveals an exceedingly sharp inner boundary for the ultrarelativistic electrons. Additional, concurrently measured data¹¹ reveal that this barrier to inward electron radial transport does not arise because of a physical boundary within the Earth's intrinsic magnetic field, and that inward radial diffusion is unlikely to be inhibited by scattering by electromagnetic transmitter wave fields. Rather, we suggest that exceptionally slow natural inward radial diffusion combined with weak, but persistent, wave-particle pitch angle scattering deep inside the Earth's plasmasphere can combine to create an almost impenetrable barrier through which the most energetic Van Allen belt electrons cannot migrate.

Figure 1 shows that over the first 20 months (1 September 2012 to 1 May 2014) of NASA's Van Allen Probes¹¹ mission lifetime, highly relativistic and ultrarelativistic electrons were present in substantial (but highly variable) numbers at a distance corresponding to a McIlwain $L \gtrsim 3$. (L is the distance in Earth radii for a magnetic field line to cross the magnetic equatorial plane in a static magnetic field model.) However, such electrons were not discernibly present at lower L values. In fact, earlier observations made by instruments on the Combined Release and Radiations Effects Satellite¹² and by the Solar, Anomalous, and Magnetospheric Particle Explorer^{13–15} mission suggested that the slot region and the inner zone can be filled with electrons many megaelectronvolts in energy only following the most extreme solar wind driving conditions.

Figure 1 shows that none of the solar wind driving events (Fig. 1f, g) during the Van Allen Probes operational era transported electrons (~ 2 to ~ 10 MeV) into the region with $L < 2.8$. Also, only very occasionally did the measured plasmopause boundary ever get forced inwards as close to the Earth as $L \approx 3$ (Fig. 1c). For most of the past two years, the plasmopause has been situated beyond $L \approx 4$. The operational period of the Van Allen Probes missions has been relatively quiet geomagnetically, and the plasmasphere region often extended outwards to $L \approx 5$ or farther. Thus, contrary to prior expectations, the inner edge of the highly relativistic electron population measured by the Relativistic Electron-Proton

Telescope (REPT) on board each of the two probe spacecraft (Fig. 1c) was rarely collocated with the plasmopause. Instead, an almost complete lack of very high-energy electrons (in a region of slot morphology) was seen only (but persistently) for $L < 2.8$ (Fig. 1a–e).

Figure 2 shows that the inner boundary of ultrarelativistic (~ 7.2 MeV) electron trapping is extremely sharp and stable for many months. Even when external solar wind driver events cause erosion of some part of the higher- L population, as on 2 September 2012 (Fig. 2a) or 1 March 2013 (Fig. 2b), the ultrarelativistic electrons remained persistently high in intensity for $L > 2.8$ and showed no measurable flux for $L < 2.8$. Furthermore, as shown in Fig. 2c, when a solar wind shock wave impinged on the magnetosphere and drove the 7.2 MeV electrons inwards in a step-like fashion on 1 October 2013, these extremely high-energy electrons moved inwards only in such a way as to again have their inner boundary at $L \approx 2.8$.

As shown in Fig. 3a–c, a sampling at 31 d intervals of radial profiles of particle fluxes over much of the Van Allen Probes lifetime shows no instance of any highly relativistic electrons migrating inwards of $L = 2.8$. The data also reveal that the boundary tends to become sharper (that is, have a steeper gradient of flux versus L) at higher electron energies. Furthermore, surveys of concurrently measured plasmaspheric hiss occurrence (Fig. 3d) from the Electric and Magnetic Field Instrument Suite and Integrated Science (EMFISIS) instrument¹⁶ on board the probe spacecraft show no sharp boundary or radial gradient change at $L = 2.8$ for these electromagnetic waves. Thus, the presence of such a clear, persistent and seemingly impenetrable barrier to inward transport of ultrarelativistic electrons at this very specific location presents a substantial puzzle.

Multi-megaelectronvolt electron losses result from processes that scatter a particle's pitch angle into the atmospheric loss cone. For example, Earth's magnetic field exhibits the South Atlantic Anomaly (SAA), a region of weaker magnetic field strengths in a low-altitude region east of South America¹⁷. The effects of the expanded atmospheric loss cone associated with the SAA are centred near $L \approx 1.5$, with smaller magnetic perturbations extending outwards to $L > 3$. Therefore, precipitation of energetic electrons into the SAA would not be expected to produce the sharp boundary in trapped electrons observed at $L = 2.8$. Space weather monitoring sensor data from the Van Allen Probes confirm the presence of this sharp boundary (Extended Data Fig. 1). Data from a small, low-altitude spacecraft, the Colorado Student Space Weather Experiment (Extended Data Fig. 2), further confirm the view that an inward boundary exists at $L \approx 2.8$ for $E > 3.8$ MeV electrons that is quite separate from concurrently identified SAA effects.

Another possible reason for the region of trapped electrons to have a sharp inward boundary could relate to the precipitation of energetic electrons induced by ground-based radio transmitters. Early work^{18,19} supported the view that powerful, very low-frequency (VLF) radio transmitters at fixed locations on Earth's surface could cause substantial loss

¹Laboratory for Atmospheric and Space Physics, University of Colorado, Boulder, Colorado 80303, USA. ²Department of Atmospheric and Oceanic Sciences, University of California, Los Angeles, California 90095, USA. ³Massachusetts Institute of Technology, Haystack Observatory, Westford, Massachusetts 01886, USA. ⁴Aerospace Corporation Space Sciences Lab, Los Angeles, California 90009, USA. ⁵School of Physics and Astronomy, University of Minnesota, Minneapolis, Minnesota 55455, USA. ⁶NASA Goddard Space Flight Center, Greenbelt, Maryland 20771, USA. ⁷Department of Physics, University of Iowa, Iowa City, Iowa 52242, USA. ⁸Center for Solar-Terrestrial Research, New Jersey Institute of Technology, Newark, New Jersey 07102, USA.

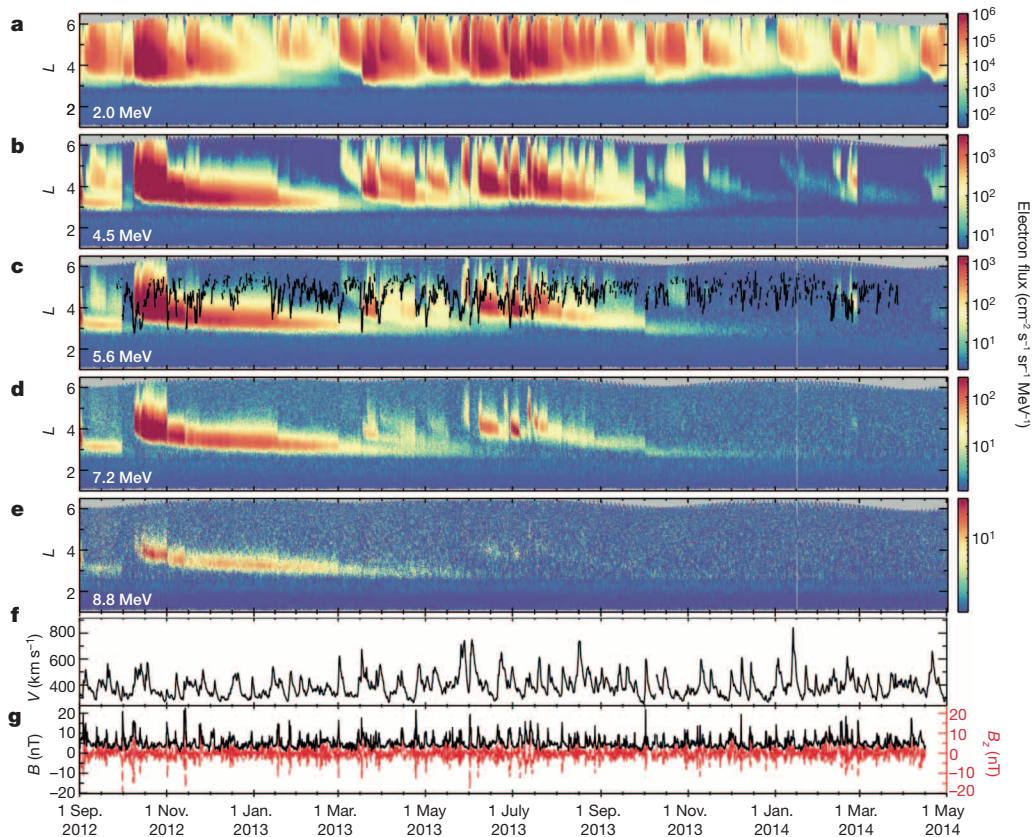


Figure 1 | A 20-month overview of electron fluxes within the Earth's Van Allen radiation belts. **a–e**, REPT-A instrument data²⁶ from initial instrument turn-on (1 September 2012) until 1 May 2014. Each panel corresponds to a different electron energy, as shown, and is plotted as a representation of electron differential-spin-averaged fluxes colour-coded as indicated. The data are shown as functions of L on the vertical axis and time along the horizontal axis. Each panel shows electron measurements from $L = 1.0$ to ~ 6.5 as covered by the highly elliptical Van Allen Probes¹¹ orbits. By comparison with similar plots of data from the same instruments in earlier studies⁷, there is a smaller flux of energetic electrons for $L < 2$. This reflects a substantially improved REPT processing algorithm to remove background due to very

intense inner-zone proton fluxes in all the electron channels⁹. **f, g**, The concurrently measured solar wind speed (**f**), black; north–south component (B_z), red (**g**) upstream of the Earth. The broken black trace plotted over the REPT data in **c** shows the measured location of the plasmapause. This plasmapause location is derived from spacecraft potential measurements¹¹, which can be used as a proxy for local plasma density. We note that in **a–e** the highly energetic electrons measured by REPT sensors throughout the mission never seem to extend inwards of $L \approx 2.8$. This forms a particularly clear and sharp boundary for the ultrarelativistic electrons as shown in **c–e**.

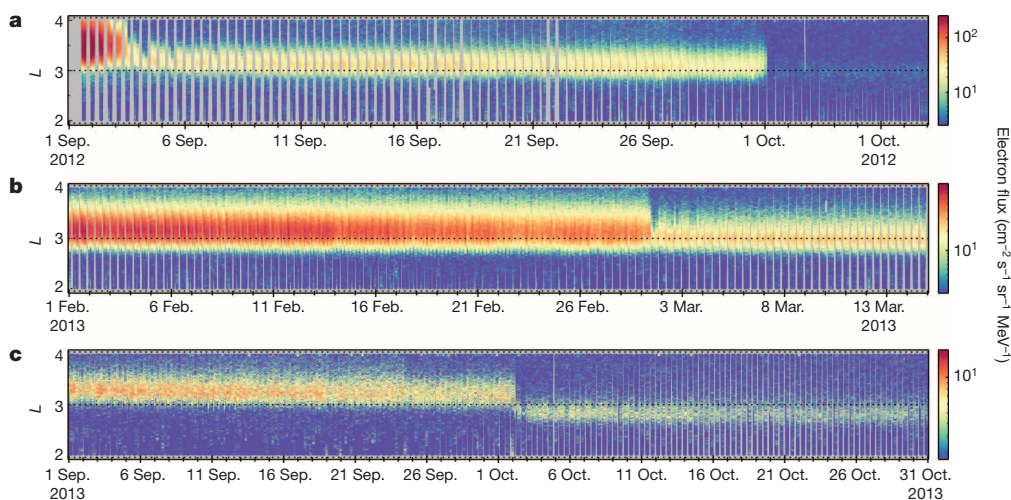


Figure 2 | Electron colour-coded data showing the sharp inner edge observed for ultrarelativistic electrons. These plots are similar to the format of Fig. 1a–e, but including the combined data from REPT-A and REPT-B²⁶. The focus in this figure is upon 7.2 MeV (6.7–7.7 MeV) electrons (Fig. 1d). **a**, Sharp inner edge as seen in the L –time format for 1 September 2012 to 30 September 2013. This relativistic electron ‘storage ring’ disappeared suddenly on 30 September 2012⁷, but before then the 7.2 MeV electrons never migrated

inwards of $L = 2.8$. **b**, Similar to **a**, but showing REPT data from 1 February 2013 to 15 March 2015. Throughout this period, the inner edge of the region of 7.2 MeV electrons did not deviate from $L = 2.8$. **c**, Similar to **a**, but for the period from 1 September to 31 October 2013. From 1 September to 1 October, the 7.2 MeV electron fluxes slowly moved inwards towards $L = 3.0$. On 1 October, an abrupt solar wind transient (shock wave) drove the storage ring inwards to a new equilibrium position with the inner edge once again at $L \approx 2.8$.

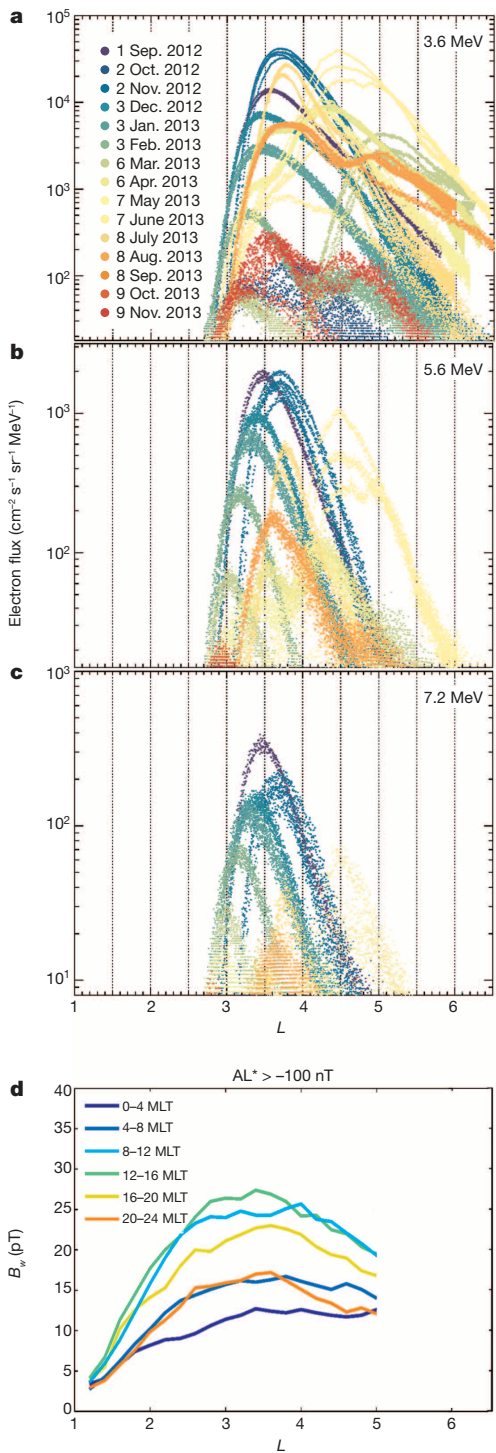


Figure 3 | Electron flux radial profiles for selected outer Van Allen zone passages. Each colour-coded profile shows the differential directional flux measured by the REPT-A instrument during a passage of a Van Allen Probe spacecraft through the magnetosphere. Passes are chosen at 31 d intervals to sample the radiation belt properties under a wide variety of conditions throughout the mission lifetime. **a**, Sampled passes for the 3.6 MeV (3.2–4.0 MeV) REPT energy channel. **b**, Similar to **a**, but for the 5.6 MeV (5.0–6.2 MeV) REPT energy channel. **c**, Similar to **a**, but for the 7.2 MeV (6.7–7.7 MeV) energy channel. In all cases, the high-energy electron profiles never extend significantly inwards of $L = 2.8$. Also, the spatial flux gradients at the inner edge of the outer Van Allen belt tend to become steeper as energy increases. **d**, Statistical survey of plasmaspheric hiss occurrence frequency for the period of the Van Allen Probes mission (based on EMFISIS data (ref. 16)). No sharp boundary is seen at $L = 2.8$ (or elsewhere) in the radial occurrence distributions of the hiss. AL^* is the minimum of the auroral electrojet index within the previous 3 h time period, derived from geomagnetic variations in ground magnetometer chain data. B_w is the magnetic field intensity of the hiss wave, and MLT is magnetic local time.

Fig. 3) show no evidence of any sharp or discontinuous features in the angular distributions that might be associated with geophysical boundaries or localized sources of wave interactions.

As further shown in Extended Data Fig. 4, REPT-measured electron fluxes always peak at 90° pitch angles as the spacecraft remain near the magnetic equatorial plane (the spacecraft orbits have a 10° inclination). Therefore, strong scattering and isotropization is not evident in the data. The scattering lifetimes of highly relativistic electrons inside the plasma-pause are very long (Fig. 4), and so we do not believe that the observed sharp inner edge is due to some anomalous fast loss process. Thus, we conclude that the persistent inner edge represents a remarkably stable boundary where weak scattering losses are dominant over even weaker radial diffusion transport (Fig. 4). The fact that the inner edge can move abruptly during solar disturbances (Fig. 2) suggests that its location can be changed either by a pronounced increase in the radial diffusion rate or by further local acceleration.

The inner edge of the relativistic electron population is a remarkable feature at all geographic longitudes (Extended Data Fig. 5). It has not

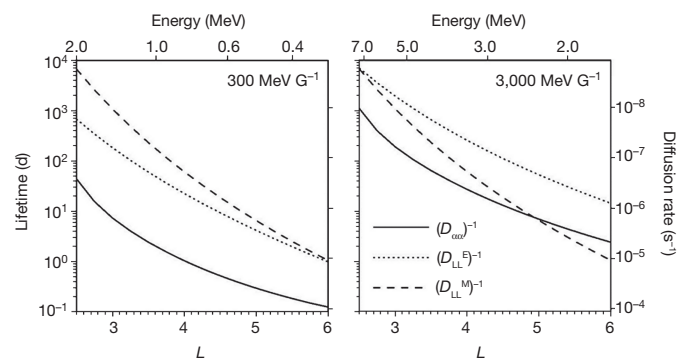


Figure 4 | A comparison between the timescales for scattering loss and inward radial diffusion. The lifetime $(D_{\alpha\alpha})^{-1}$ of energetic electrons due to pitch angle scattering by plasmaspheric hiss under weak-to-moderate geomagnetic activity (Fig. 3d), plotted (solid lines) as a function of L for two representative magnetic moments, 300 and 3,000 MeV G^{-1} . Corresponding electron energies are shown along the top axis. The rates of inward radial diffusion and the corresponding transport timescales due to ultralow-frequency fluctuating electric $(D_{LL}^E)^{-1}$ and magnetic $(D_{LL}^M)^{-1}$ fields, based on the parameterization of ref. 27, are shown as dotted and dashed lines, respectively. For the ultrarelativistic population (3,000 MeV G^{-1}), the timescale for radial transport inside $L \approx 3$ exceeds 1,000 d, whereas the scattering loss time is comparable to 100 d. Consequently, any ultrarelativistic electrons that are injected near $L \approx 3$ will remain in place subject only to very slow loss to the atmosphere, thus accounting for the remarkable stability of the inner edge of the ultrarelativistic rings. The lower-energy electron population ($< 1 \text{ MeV}$) near $L \approx 3$ should decay much more rapidly, on a timescale of $< 10 \text{ d}$. This is also consistent with recent observations made using the Van Allen Probes²².

of otherwise stably trapped inner-zone electrons in the 100–500 keV energy range. Although some VLF transmitter power can leak into the inner magnetosphere, previous detailed analyses have shown¹⁹ that VLF wave interactions (due to Doppler-shifted cyclotron resonances) from ground transmitters would only be substantial for electrons with energies $< 0.5 \text{ MeV}$ and would be expected to be important only at mid-latitude locations where $L < 2$. We conclude that such man-made signals do not have a substantial effect on the ultrarelativistic particles (which should instead be much more efficiently scattered by lower-frequency hiss at $L \approx 2.8$ (ref. 20)). Thus, we do not believe that the sharp boundary of electron trapping at $L = 2.8$ described above for ultrarelativistic electrons is related to VLF radio transmitters or to special features in the geomagnetic field. Moreover, REPT pitch angle plots (Extended Data

previously been discussed in the literature because we have never previously had such accurate measurements at high energies. However, this inner edge being at such low L , well inside the plasmapause, seems to require that electron acceleration occur just outside this location. The radial transport of such electrons from the heart of the outer zone to $L \approx 2.8$ is usually very slow⁵ (on the timescale of years). Thus, the electrons would be significantly depleted (by several orders of magnitude) by wave scattering during inward transport from the nominal plasmapause location at around four to five Earth radii (Fig. 4). Unless there occurs a prompt interplanetary-shock-induced acceleration like the March 1991 event²¹, we would favour a local wave acceleration process that occurs just outside the plasmapause^{8,22} when the plasmapause is pushed into the lower- L region.

At present, we contend that the plasmapause location has a role in the formation of the inner edge, and that this requires a strong solar wind event to cause both the plasmasphere to erode through convection and the plasmapause to move to lower L . But once the ultrarelativistic electron population is formed at such low L , it will stay in place subject only to very slow decay on a timescale of 100 d (refs 23, 24). These results therefore demonstrate that extraordinarily strong spatial gradients can be maintained for quite long times in ultrarelativistic electron-trapping geometries. This has potential relevance both for plasma physics and for non-terrestrial cosmic systems that magnetically confine highly energetic particles²⁵.

Online Content Methods, along with any additional Extended Data display items and Source Data, are available in the online version of the paper; references unique to these sections appear only in the online paper.

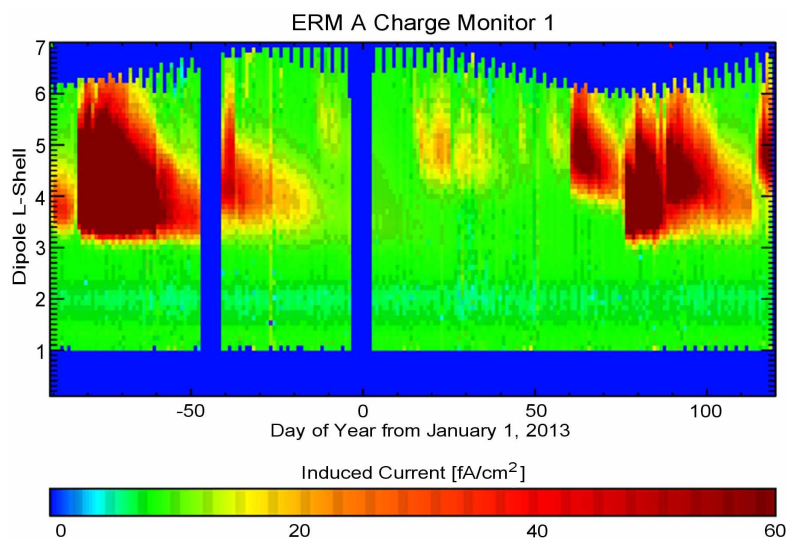
Received 18 June; accepted 10 October 2014.

- Van Allen, J. A., Ludwig, G. H., Ray, E. C. & McIlwain, C. E. Observation of high intensity radiation by satellites 1958 alpha and gamma. *Jet Propuls.* **28**, 588–592 (1958).
- Van Allen, J. A. & Frank, L. A. Radiation around the Earth to a radial distance of 107,400 km. *Nature* **183**, 430–434 (1959).
- Johnson, M. H. & Kierein, J. Combined Release and Radiation Effects Satellite (CRRES): spacecraft and mission. *J. Spacecr. Rockets* **29**, 556–563 (1992).
- Blake, J. B., Baker, D. N., Turner, N., Ogilvie, K. W. & Lepping, R. P. Correlation of changes in the outer-zone relativistic electron population with upstream solar wind and magnetic field measurements. *Geophys. Res. Lett.* **24**, 927–929 (1997).
- Lyons, L. R. & Thorne, R. M. Equilibrium structure of radiation belt electrons. *J. Geophys. Res.* **78**, 2142–2149 (1973).
- Li, X., Baker, D. N., O'Brien, P., Xie, L. & Zong, Q. G. Correlation between the inner edge of outer radiation belt electrons and the innermost plasmapause location. *Geophys. Res. Lett.* **33**, L14107 (2006).
- Baker, D. N. *et al.* A long-lived relativistic electron storage ring embedded in Earth's outer Van Allen belt. *Science* **340**, 186–190 (2013).
- Thorne, R. M. *et al.* Rapid local acceleration of relativistic radiation belt electrons by magnetospheric chorus. *Nature* **504**, 411–414 (2013).
- Baker, D. N. *et al.* The Relativistic Electron-Proton Telescope (REPT) instrument on board the Radiation Belt Storm Probes (RBSP) spacecraft: characterization of Earth's radiation belt high-energy particle populations. *Space Sci. Rev.* **179**, 337–381 (2013).
- Spence, H. E. *et al.* Science goals and overview of the Radiation Belt Storm Probes (RBSP) Energetic Particle, Composition, and Thermal Plasma (ECT) suite on NASA's Van Allen Probes mission. *Space Sci. Rev.* **179**, 311–336 (2013).
- Mauk, B. H. *et al.* Science objective and rationale for the Radiation Belt Storm Probes mission. *Space Sci. Rev.* **179**, 3–27 (2013).
- Blake, J. B., Kolasinski, W. A., Fillius, R. W. & Mullen, E. G. Injection of electrons and protons with energies of tens of MeV into $L < 3$ on March 24, 1991. *Geophys. Res. Lett.* **19**, 821–824 (1992).
- Baker, D. N. *et al.* An extreme distortion of the Van Allen belt arising from the 'Halloween' solar storm in 2003. *Nature* **432**, 878–881 (2004).
- Baker, D. N., Kanekal, S. G., Horne, R. B., Meredith, N. P. & Glauert, S. A. Low-altitude measurements of 2–6 MeV electron trapping lifetimes at $1.5 \leq L \leq 2.5$. *Geophys. Res. Lett.* **34**, L20110 (2007).
- Zhao, H. & Li, X. Inward shift of outer radiation belt electrons as a function of Dst index and the influence of the solar wind on electron injections into the slot region. *J. Geophys. Res. Space Phys.* **118**, 756–764 (2013).
- Kletzing, C. A. *et al.* The Electric and Magnetic Field Instrument Suite and Integrated Science (EMFISIS) on RBSP. *Space Sci. Rev.* **179**, 127–181 (2013).
- Roederer, J. G. *Dynamics of Geomagnetically Trapped Radiation* (Springer, 1970).
- Vampola, A. L. & Kuck, G. A. Induced precipitation of inner zone electrons, 1. Observations. *J. Geophys. Res.* **83**, 2543–2551 (1978).
- Koons, H. C., Edgar, B. C. & Vampola, A. L. Precipitation of inner zone electrons by Whistler mode waves from the VLF transmitters UMS and NWC. *J. Geophys. Res.* **86**, 640–648 (1981).
- Abel, R. W. & Thorne, R. M. Electron scattering loss in Earth's inner magnetosphere: 1. Dominant physical processes. *J. Geophys. Res.* **103**, 2385–2396 (1998).
- Li, X. *et al.* Simulation of the prompt energization and transport of radiation particles during the March 23, 1991 SSC. *Geophys. Res. Lett.* **20**, 2423–2426 (1993).
- Baker, D. N. *et al.* Gradual diffusion and punctuated phase space density enhancements of highly relativistic electrons: Van Allen Probes observations. *Geophys. Res. Lett.* **41**, 1351–1358 (2014).
- Ni, B., Bortnik, J., Thorne, R. M., Ma, Q. & Chen, L. Resonant scattering and resultant pitch angle evolution of relativistic electrons by plasmaspheric hiss. *J. Geophys. Res.* **118**, 7740–7751 (2013).
- Thorne, R. M. *et al.* Evolution and slow decay of an unusual narrow ring of relativistic electrons near $L \sim 3.2$ following the September 2012 magnetic storm. *Geophys. Res. Lett.* **40**, 3507 (2013).
- Eastlund, B. J., Miller, B. & Michel, F. C. Emission from closed and filled magnetospheric shells and its application to the Crab pulsar. *Astrophys. J.* **483**, 857–867 (1997).
- NASA Goddard Space Flight Center. Coordinated Data Analysis Web, http://cdaweb.gsfc.nasa.gov/istp_public/ (11 September 2014).
- Brautigam, D. H. & Albert, J. Radial diffusion analysis of outer radiation belt electrons during the October 9, 1990 magnetic storm. *J. Geophys. Res.* **105**, 291–309 (2000).

Acknowledgements We thank the entire Van Allen Probes mission team for suggestions about this work. Data access was provided through the Johns Hopkins University/Applied Physics Lab Mission Operations Center and the Los Alamos National Laboratory Science Operations Center. This work was supported by JHU/APL contract 967399 under NASA's prime contract NAS5-01072. All Van Allen Probes data used are publicly available at <http://www.rbbsp-ect.lanl.gov>.

Author Contributions D.N.B. developed the project, directed the data analysis and was primarily responsible for writing the paper. A.N.J., V.C.H. and S.G.K. analysed REPT data and produced related figures. R.M.T. provided theoretical guidance. J.C.F. and P.J.E. provided ground-based data for context. J.F.F. provided access to supplementary Van Allen Probes particle data. X.L., L.B. and Q.S. provided REPTile data. D.M.M. provided plasmapause location from EFW data. J.R.W. provided electric field data and W.K. provided EMFISIS data access. W.L. performed hiss data statistical analysis. Q.M. performed particle scattering and diffusion lifetime calculations. A.G. and L.J.L. provided ERM data from the Van Allen Probes mission.

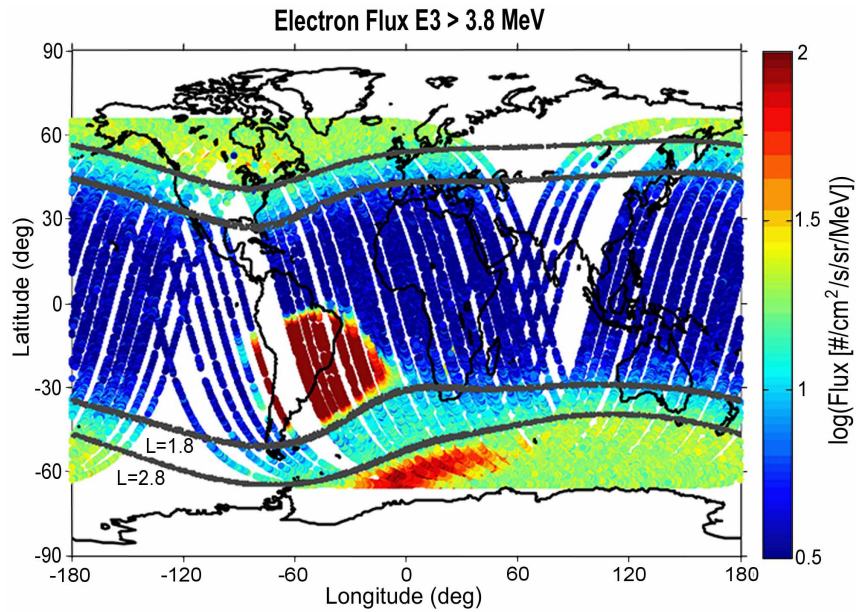
Author Information Reprints and permissions information is available at www.nature.com/reprints. The authors declare no competing financial interests. Readers are welcome to comment on the online version of the paper. Correspondence and requests for materials should be addressed to D.N.B. (daniel.baker@lasp.colorado.edu).



Extended Data Figure 1 | Induced charge monitor current density measured by Van Allen Probes spacecraft A. The first seven months of the mission are shown as a function of dipole L shell. Time is measured from 1 January 2013. The charge plate of the Environmental Radiation Monitor²⁸ (ERM) from which the data shown here were acquired consists of a 10 cm^2 plate under 1 mm-thick aluminium, and is thus able to detect penetrating electrons

of more than 0.7 MeV and protons of more than 15 MeV. Note that no enhanced charging was observed below $L \approx 3$ for solar active periods throughout October 2012 (about day -80) and April 2013 (about day $+80$). Similar results (not shown) were observed in charge monitor 2, which was under 3.8 mm of aluminium and was thus able to detect penetrating electrons of more than 2 MeV and protons of more than 30 MeV.

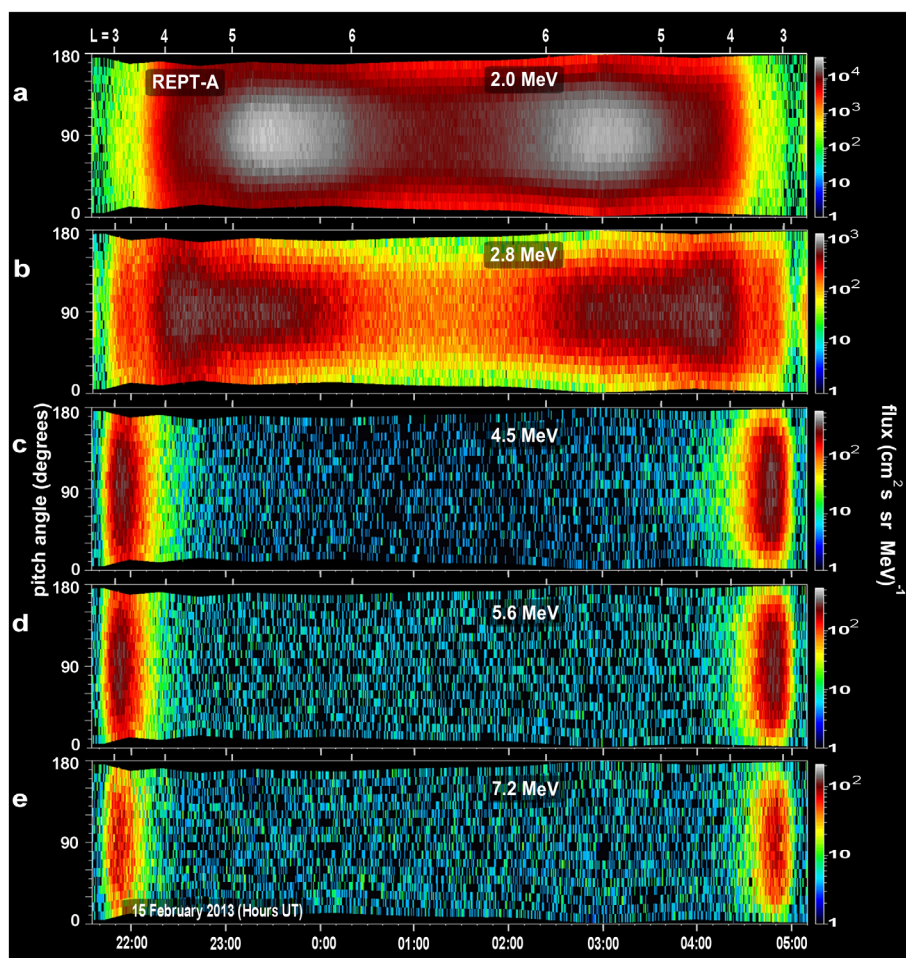
28. Goldsten, J. O. *et al.* The Engineering Radiation Monitor for the Radiation Belt Storm Probes Mission. *Space Sci. Rev.* **179**, 485–502 (2013).



Extended Data Figure 2 | Data from the Colorado Student Space Weather Experiment CubeSat²⁶ mission in low-Earth orbit. The REPT integrated little experiment (REPTile) >3.8 MeV electron data are portrayed in

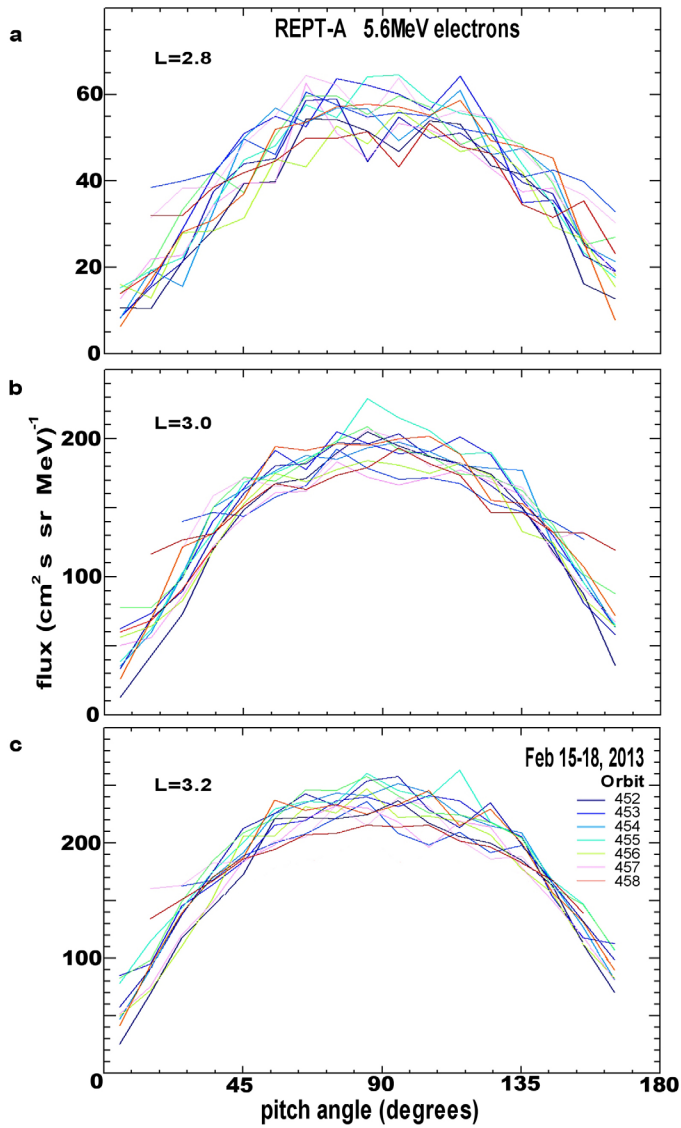
a latitude–longitude Mercator projection format showing that the electron inner edge of the outer zone is well separated from the SAA (which is dominated for this energy range in REPTile by inner-zone protons)²⁹.

29. Li, X. *et al.* First results from CSSWE CubeSat: characteristics of relativistic electrons in the near-Earth environment during the October 2012 magnetic storms. *J. Geophys. Res. Space Phys.* **118**, 6489–6499 (2013).

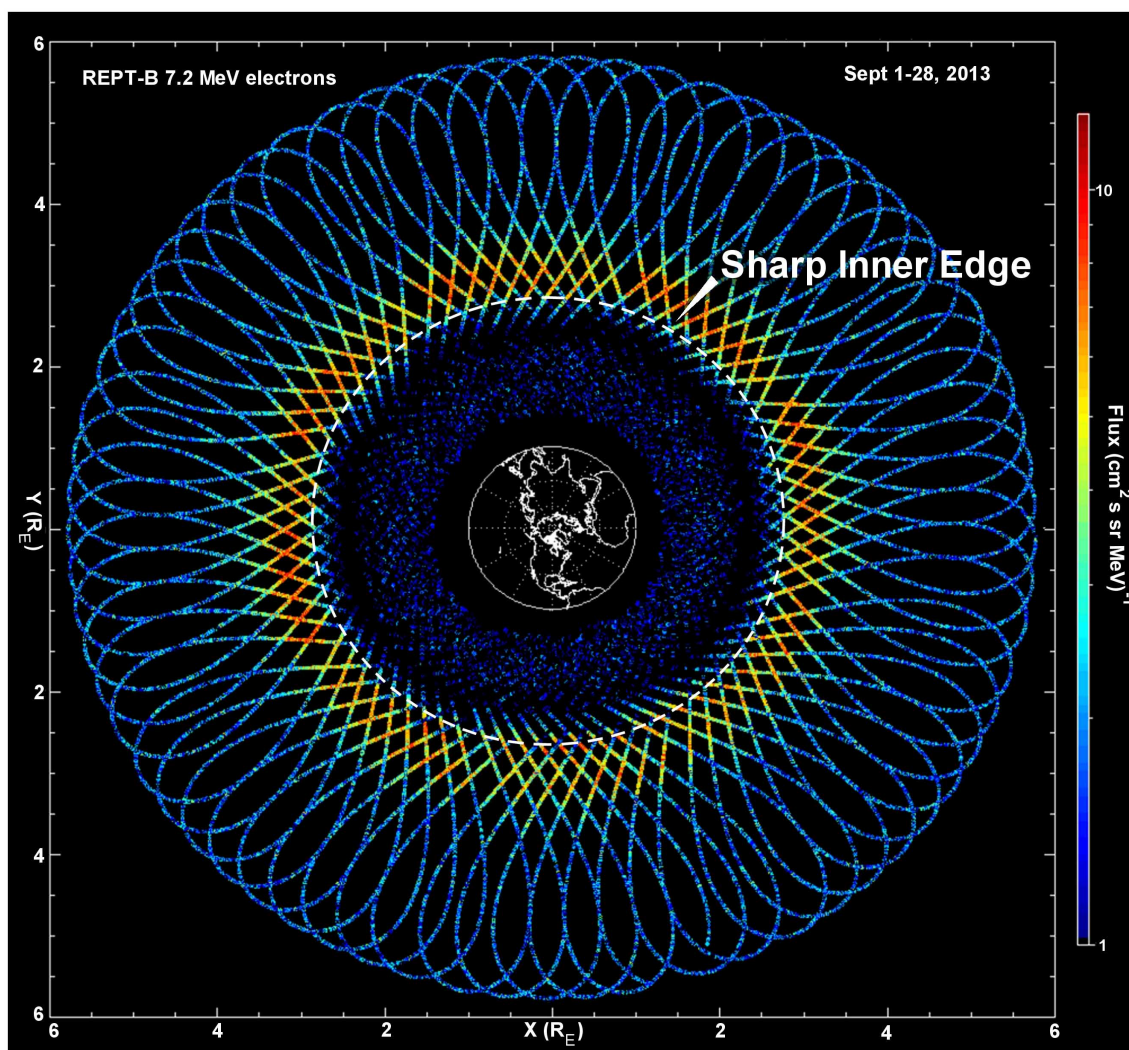


Extended Data Figure 3 | Pitch angle data exhibiting the behaviour of high-energy-electron angular distributions. This figure shows illustrative data²⁶ in the storage ring region and at the inner edge of the outer zone for an entire Van Allen Probe A orbital pass for February 2013 from 21:30 UT on

15 February to about 5:00 UT on 16 February. **a**, Colour-coded directional fluxes for 2.0 MeV electrons. **b**, Similar data for 2.8 MeV electrons. **c**, Similar data for 4.5 MeV electrons. **d**, Similar data for 5.6 MeV electrons. **e**, Similar data for 7.2 MeV electrons.



Extended Data Figure 4 | Differential directional flux values versus pitch angle values. Data measured by REPT-A for 15–18 February 2013 for different spacecraft orbit numbers are colour-coded according to the inset in **c**. **a**, Distributions seen right at the inner edge of the trapping boundary at $L = 2.8$. **b**, Distributions taken in the higher-flux regions at $L = 3.0$. **c**, Distributions taken even further out in the trapping region at $L = 3.2$.



Extended Data Figure 5 | A colour-coded geographic representation of ultrarelativistic electron fluxes. The orbital tracks of Van Allen Probe B for the REPT-B sensor fluxes from 1 September to 28 September 2013 are projected onto the geographical equatorial plane. As the spacecraft precesses in its elliptical orbit around the Earth, it forms a ‘Spirograph’ pattern in the geographically fixed, Earth-centred coordinate system. The resulting orbital pattern shows the relatively stable (during this 4-week period) band of 7.2 MeV

electrons from a radius of about 2.8 Earth radii (R_E) out to about $3.5R_E$. Inside $2.8R_E$ there is an almost complete absence of electrons, resulting in the slot region. Note also that there is hardly any discernible population of electrons at these energies in the inner zone ($L \leq 2$) during this period. The superimposed circle at $2.8R_E$ shows how sharp and distinctive the inner boundary is for ultrarelativistic electrons and how generally symmetric this boundary is all around the Earth.